Malaysian Journal of Chemistry, 2023, Vol. 25(3), 481-491
(Special Issue: *3rd IKMPB Online Symposium 2023 - Innovation in Chemistry Towards Sustainable Development*)

Synthesis, Characterization, Antimicrobial Activity and ADMET Analysis of *S*-benzyl-α-*N*-(anisoyl)-dithiocarbazate and Its Metal Complexes

Siti Khadijah Roslan, How N. -F Fiona* and Nurasyikin Hamzah
Department of Chemistry, Kulliyyah of Science, International Islamic University Malaysia (IIUM)
25200, Kuantan, Pahang, Malaysia
*Corresponding author (e-mail: howfiona@iium.edu.my)

Dithiocarbazate derivatives have shown significant bioactivities especially as antibacterial agents. However due to the poor penetration into bacteria and its toxicity, their potential as a good antibacterial agent was dismissed. Therefore, the purpose of this study was to synthesize a new substituted dithiocarbazate derivative, *S*-benzyl-α-*N*-(anisoyl) dithiocarbazate (SB4OME) and its metal complex. SB4OME behaves as a tridentate chelating agent that coordinates with the metal ions with the general formula of $[M(SB4OME)_2]$ where M is Cu^{2+}, Zn^{2+}, Co^{2+} and Ni^{2+}. All the compounds were characterized with various physico-chemical techniques including melting point analysis, FT-IR spectroscopy, UV–Vis spectroscopy, NMR spectroscopy, magnetic susceptibility and molar conductivity measurements. The antibacterial activity of all the compounds was tested against *Staphylococcus aureus* (ATCC 25923), *Bacillus cereus* (ATCC 11778), *Pseudomonas aeruginosa* (ATCC 27853) and *Escherichia coli* (ATCC 25922). The complexes significantly exhibited a stronger antibacterial activity than SB4OME against specific bacteria. All compounds showed a good drug like character through ADMET investigation, which was determined using SwissADME and Pro Tox-II. This showed that SB4OME and its complexes reduced the toxicity of dithiocarbazate derivatives and significantly enhanced their penetration in bacteria due to the coordination with metal ions resulting in increased bioactivity.

Keywords: Dithiocarbazate derivatives; metal complexes; antimicrobial; ADMET

Received: January 2023; Accepted: April 2023

Dithiocarbazate derivatives have drawn much attention in recent years due to their promising bioactivities against a variety of bacteria cells [1-2]. In fact, the addition of various chemical substituents, which results in even slight structural alterations, modifies the potency of these compounds [3-4]. Although many dithiocarbazate derivatives have been reported in the literature for their bioactivities, none of them was passed to the clinical trial due to the poor penetration in bacteria and most importantly, it involves the toxicity issue. Consequently, their potential as drug candidates was dismissed.

Due to the presence of nitrogen and sulphur donor atoms in dithiocarbazate derivatives, they can form complexes with various metal ions increasing the compound's properties as a therapeutic agent [5]. Thus, to improve their penetration in bacteria, dithiocarbazates derivatives have served as a ligand to coordinate with metal ions to form metal complexes. According to the antibacterial findings [6-7], metal complexes were generally found to be more potent than their parent ligand against the tested bacterial strains. *S*-benzyl dithiocarbazates (SBDTC) is one of the most popular dithiocarbazate derivatives among researchers which have been studied for many years. Despite having excellent bioactivities, the compound was expected to be toxic mainly because of carbon disulphide (CS_2), which has also been used in the synthesis of dithiocarbamate. A preclinical study has been done on dithiocarbamate to determine its general toxicity but it was challenging to reduce the possibility of toxicity risk due to CS_2 [8]. Therefore, modifications have been made to SBDTC's structure by introducing simple organic compounds such as aldehyde, ketone, acyl halide and many more to reduce its toxicity risk.

To create safer, more potent, and more widely accessible drugs, new drugs are developed by structural modification of existing precursor compounds, which are reported to have excellent bioactivity. During the development process, it is critical to analyze factors such as absorption, distribution, metabolism, excretion, and toxicity (ADMET). These parameters play an essential role in determining the compound's potential to be developed as a bioactive molecule, which is crucial for the synthesis of potential drugs [9]. To choose the best lead compounds, specific cut-off values of certain drug-like properties have been employed as criteria such as the "Lipinski rule of 5" [10]. Malgorzata and his peers have developed ProTox-II, a web server for the prediction of toxicity which can

†Paper presented at the 3rd IKMPB Online Symposium 2023 - Innovation in Chemistry Towards Sustainable Development

be used to determine the toxicity of new drug candidates. The prediction approach is based on the similarity of compounds with known median lethal doses (LD_{50}) and includes the identification of toxic fragments [11].

Therefore, considering the facts and our persistent interest in this field, this work reports on the synthesis and characterization of SB4OME and its metal complexes. All compounds were characterized by melting point analysis, FT-IR spectroscopy, UV–Vis spectroscopy, NMR spectroscopy, magnetic susceptibility and molar conductivity measurements. They were screened for antibacterial activity against various Gram-positive and Gram-negative bacteria, namely *Staphylococcus aureus* (ATCC 25923), *Bacillus cereus* (ATCC 11778), *Pseudomonas aeruginosa* (ATCC 27853) and *Escherichia coli* (ATCC 25922). Their ADMET analysis was also done by using Swiss-ADME and Protox-II to observe the drug-likeness and toxicity of these compounds.

EXPERIMENTAL

Chemicals and Materials

All chemicals were used as purchased.

Preparation of *S*-benzyl Dithiocarbazate (SBDTC)

SBDTC was prepared as previously reported [12]. Potassium hydroxide (0.1 mol, 5.7 g) was dissolved in 35 ml cold 90% ethanol and hydrazine hydrate (0.1 mol, 5 ml) was added to this solution. The mixture was cooled down in an ice bath until the temperature reached 0 °C. To the resultant cooled solution, carbon disulphide (0.1 mol, 6 ml) was added dropwise over an hour with constant stirring using a mechanical stirrer to obtain two layers. The brown oil (lower layer) was obtained and dissolved in 30 ml cold 40% ethanol. The solution was kept in an ice bath (0-5 °C) and benzyl chloride (0.1 mol, 11.37 ml) was added dropwise with vigorous stirring. Upon the completion of benzyl chloride addition, a white precipitate was obtained, which was filtered and dried over silica gel overnight. The melting point obtained was 122-123 °C.

Preparation of *S*-benzyl-α-*N*-(anisoyl) Dithiocarbazate (SB4OME)

SB4OME was prepared according to [13]. SBDTC (0.01 mol, 1.983 g) was dissolved in 30 ml absolute ethanol, which was mixed with potassium hydroxide (0.01 mol, 0.56 g) in 10 ml ethanol. 4-methoxybenzoyl chloride (0.01 mol, 1.42 ml) was added dropwise to the solution with constant stirring and heating. After the complete addition of 4-methoxybenzoyl chloride, the resulting solution was allowed to heat and stir to reduce the volume to half. The white product was filtered while it was hot and dried over silica gel overnight. The product was recrystallized from ethanol. The melting point obtained was 140-142 ºC.

General Method for Preparation of Metal Complexes

Metal complexes were prepared based on the previous report of [13]. *S*-benzyl-α-*N*-(anisoyl) dithiocarbazate (0.0009 mol, 0.3 g) was dissolved in boiling ethanol (30 ml) which was added to a hot solution of metal salt (0.00045 mol) that dissolved in boiling ethanol (30 ml) was added to a hot solution of metal salt (0.00045 mol) dissolved in the same solvent (30 ml). The mixture was heated and stirred until the volume was reduced to half at approximately 20 minutes. The precipitate was filtered while it was hot and dried over silica gel overnight. The metal salts used are copper(II) acetate monohydrate (0.09 g), nickel(II) acetate tetrahydrate (0.11 g), zinc(II) acetate dihydrate (0.098 g) and cobalt(II) acetate tetrahydrate (0.11 g).

Physical Measurements

Melting points were determined using Electrothermal™ IA9300. The IR spectra were recorded in the range of 400-4000 cm^{-1} with KBr pellets on a FTIR Perkin Elmer (FTIR Frontier). The molar conductance of a 10^{-3} M solution of each metal complex in DMSO was measured at 26 ºC using a Eutech CON 700 conductivity meter. The UV–VIS spectra were recorded on a Shimadzu UV-1900 Series PC spectrophotometer (800–200 nm) in DMSO solution. ^{1}H NMR and ^{13}C NMR spectra were recorded in DMSO-d_6 on NMR Bruker Ultra Shield Plus 500 MHz spectrometer. Magnetic susceptibility was measured with a Sherwood Scientific MSB AUTO at 298 K.

Bioactivity

Antimicrobial activity was done at the Microbiology Laboratory of Physical Building, Kulliyah of Science, International Islamic University Malaysia.

Bacteria Culture

Four pathogenic bacteria were cultured according to reported literature [14]. All strains, *Staphylococcus aureus* (ATCC 25923), *Bacillus cereus* (ATCC 11778), *Pseudomonas aeruginosa* (ATCC 27853) and *Escherichia coli* (ATCC 25922) were stored at -80°C and streaked on Mueller-Hinton agar plates. Strains were grown at 37°C on Mueller-Hinton medium 24 hour prior to the MIC assay. Bacterial inocula were prepared by picking 3-4 colonies from the agar plate and adjusted to the 0.5 Mc Farland standard solutions in Mueller-Hinton broth. The turbidity of the bacteria was determined by the optical density (OD) using a single-beam UV-Vis Spectrophotometer at 600 nm. The ideal OD for the bacteria is 0.1, which is also equivalent to 1.5×10^{-8} CFU/mL.

Antimicrobial Assay

The antimicrobial assay was carried out by determining the minimum inhibitory concentration (MIC, mg/mL) [15]. Generally, the concentrations of the synthesized compounds and positive control (gentamycin) were prepared by two-fold serial dilutions. The concentration of 109-7000 µg/ml was prepared in DMSO in labeled test tubes. 100 µL of Muller Hinton broth was added to each well, except for the first well. After that, 200 µL of synthesized compound or positive control was added into the first well of the plate and serial dilutions were done using a micropipette. 100 µL of the fresh bacterium was added to all wells. After incubating at 37°C for 24 hours, the least concentration of the trial compounds that did not show any observable growth of microorganisms was considered as an MIC value.

ADMET Analysis

All compounds synthesized were subjected to ADMET analysis using SwissADME (http://www.swissadme.ch/) [16] and Pro-Tox II webpages (http://tox.charite.de/protox_II) [17]. The 2D structure of the synthesized compounds was sketched using ChemDraw to generate their SMILES notations and submitted for evaluation.

RESULTS AND DISCUSSION

Synthesis, physical and analytical data

Table 1 displays the physical and analytical data for SBTDC, SB4OME and its metal complexes. All suggested structures in the present report were agreed and supported by the obtained spectroscopy and analytical data. All compounds gave a good yield except for SBDTC, $Cu(SB4OME)_2$, and $Ni(SB4OME)_2$. The low yield of SBDTC occurred due to the inconsistent increase of the temperature in the synthesis. Meanwhile, the low yield of $Cu(SB4OME)_2$, and $Ni(SB4OME)_2$ occurred because the synthesis was done in a 1:1 ratio of metal and ligand reaction. In the presence of potassium hydroxide, the reaction of SBDTC with anisoyl chloride produced *S*-benzyl-α-*N*-(anisoyl)dithiocarbazate as shown in Figure 1. The thione tautomer of SBDTC is unstable in solution and is changed by enethiolization to the more stable thiolo forms [18]. By losing the proton, SBDTC behaves as a uninegatively charged weak base due to resonance involving the nonbonding pair of electrons on the nitrogen atom [19]. As a result, the anisoyl group is directed to the α-nitrogen on SBDTC, forming *S*-benzyl-α-*N*-(anisoyl)-dithiocarbazate (SB4OME) (Figure 1). SB4OME, which behaves as a uninegative charged ligand, coordinates with transition metal ions by tridentate NOS donor atom to form complexes with different colors observed.

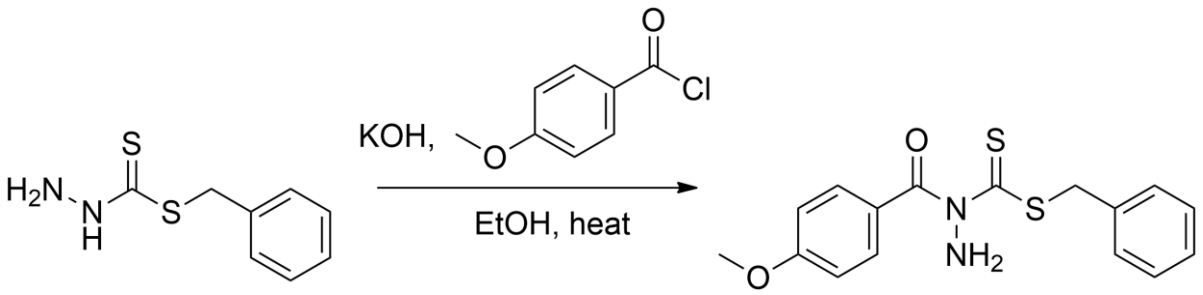

Figure 1. Reaction scheme of the formation of SB4OME.

Table 1. Physical and analytical data of SB4OME and its complexes.

Compound	*Colour*	*M.p (ºC)*	*Yield (%)*
SBDTC	White	122-123	57
SB4OME	Cream	140-142	70
$Cu(SB4OME)_2$	Black	296-297	46
$Zn(SB4OME)_2$	White	265-266	72
$Co(SB4OME)_2$	Green	269-270	73
$Ni(SB4OME)_2$	Brown	260-261	54

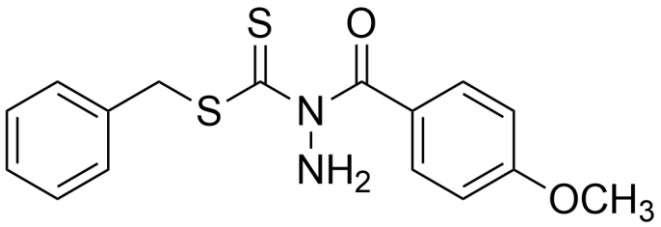

Figure 2. Molecular structure of SB4OME in thione form.

Infrared Spectroscopy Spectra

Table 2 depicts the important absorption bands in the IR spectra of these compounds. In the SB4OME spectrum, υ(N-H) bands associated with the free amine group in SBDTC were found at 3329 cm^{-1} and 3257 cm^{-1}, which is attributed to primary υ(N–H). The presence of these peaks proves that the anisoyl group is directed to the α-nitrogen on SBDTC, generating *S*-benzyl-α-*N*-(anisoyl) dithiocarbazate. In addition to absorption bands that are similar to those found in SBDTC, the spectra of SB4OME exhibit sharp and strong υ(C=O) at 1658 cm^{-1}. Both SBDTC and SB4OME exhibit significant bands showing υ(C=S) at 1048 cm^{-1} and 1043 cm^{-1}, respectively. The absence of υ(S-H) at about 2603–2707 cm^{-1} and υ(O-H) from SB4OME's IR spectra demonstrates that it exists as thione tautomer mainly in the solid state (Figure 2). For dithiocarbazate derivatives, such as SBDTC, it can undergo thione-thiol tautomerism to become stable [20]. However, for SB4OME, it can only exist in thione form due to the absence of α-hydrogen. The stable thiol tautomer occurred only when at least one proton adjacent to the α-amine group is present [2].

All SB4OME's complexes showed a similar FTIR pattern with the disappearance of one peak from primary υ(N-H) around 3300 cm^{-1} showing that the coordination occurred through the proton of the amino group. This is further confirmed by the shifting of SB4OME υ(N–N) at 1339 cm^{-1} to lower frequencies in all complexes around 1305 cm^{-1}. The complexes also had a significant negative shift in the υ(C=O) and υ(C=S) bands, demonstrating the involvement of carbonyl oxygen and thione sulphur in the coordination with the metal. In addition, the υ(S-C-S) in the complexes is found to be in the range of 959-971 cm^{-1} which is at lower wavenumbers in comparison with the SB4OME which is at 1016 cm^{-1}. Hence, SB4OME loses one proton on complexation, thus acting as a uninegative tridentate ligand to form the complexes (Figure 3).

Nuclear Magnetic Resonance Spectra

^{1}H and ^{13}C NMR data of SB4OME was reported in Table 3. The primary N-H group is responsible for the signal at δ_H = 10.551 ppm supporting the direction of the anisoyl group to the α-nitrogen on SBDTC. The resonance peaks corresponding to the aromatic groups were seen in the region of δ_H = 7.042–7.87 ppm. The methylene proton and methyl proton of the methoxy group were observed at δ_H = 4.453 and 3.833 ppm respectively. SB4OME exists as in thione form in the solution was proved by the absence of S-H proton and O-H in the ^{1}H NMR spectrum. Furthermore, the appearance of C=O and C=S in the ^{13}C NMR spectrum also supports that SB4OME exists as thione form in solution. This showed that a combination of IR and NMR spectra verify that SB4OME formed through the conjugation of anisoyl group to the α-nitrogen on SBDTC and it mainly presents as thione form in the solid and solution. Metal complexes were not sent for NMR analyses as they do not dissolve in any of the deuterated solvent.

Table 2. Selected IR bands of SBDTC, SB4OME and its metal complexes.

Compound	***IR bands (cm^{-1})***				
	υ(N–H)	υ(C=S)	υ(S-C-S)	υ(C=O)	υ(N–N)
SBDTC	3304, 3180	1048	952	-	1347
SB4OME	3329, 3257	1043	1016	1658	1339
$Cu(SB4OME)_2$	3213	1029	963	1606	1305
$Zn(SB4OME)_2$	3212	1028	966	1606	1305
$Co(SB4OME)_2$	3212	1028	959	1606	1305
$Ni(SB4OME)_2$	3209	1028	971	1606	1304

Table 3. ^{1}H-NMR and ^{13}C-NMR spectral data for SB4OME.

Compound	***^{1}H-NMR, δ (ppm)***				***^{13}C-NMR, δ (ppm)***				
	NH_2	S-CH_2	O-CH_3	Aromatic proton	C=S	C=O	O-CH_3	S-CH_2	Aromatic carbon
SB4OME	*s*, 2H (10.5)	*s*, 2H (4.4)	*s*, 3H (3.8)	*d*, (7.8-7.5, J = 6.0 Hz, 4H) *m*, (7.4-7.0, J = 7.5 Hz, 5H)	189.6	169.2	56.2	37.8	165.1-112.5

Conductivity Data

The molar conductivity of all metal complexes as shown in Table 4 are in the range of 31.4-37.8 ohm^{-1} mol^{-1} cm^2 indicating that these complexes are non-electrolytic in nature. This is in accordance with the fact that conductivity values for a nonelectrolyte are below 50 ohm^{-1} mol^{-1} cm^2 in DMSO solution [21]. Therefore, all complexes do not dissociate in solution indicating that SB4OME are directly attached to the metal ions [22-23]. Thus, SB4OME must be acting as a uninegatively charged tridentate species.

Magnetic Moment

To obtain further structural information on the metal complexes, the magnetic moments were measured and the results were tabulated in Table 4. Among all the complexes synthesized, only Zn(II) complex shows zero value for magnetic moment indicating the diamagnetic properties due to the d^{10} electron configuration [24]. The diamagnetic Zn(II) complex was expected to be six-coordinated and have an octahedral structure. The value of the effective magnetic moment of Cu(II), Co(II) and Ni(II) complexes were 1.648, 4.740 and 2.385 Bohr magneton (B.M) respectively confirming the paramagnetic characteristic of these complexes. $Cu(SB4OME)_2$ showed magnetic moments of 1.648 B.M indicating one unpair electron. Hence, it is expected to have an octahedral geometry around the copper(II) ion [25]. According to the magnetic moment of cobalt(II) complex, it was expected that the cobalt(II) ion in $Co(SB4OME)_2$ would be surrounded by an octahedral geometry [23]. Paramagnetic $Ni(SB4OME)_2$ showed magnetic moment values of 2.385 BM indicating two unpaired electron configurations which suggest an octahedral geometry [26]. Thus, all SB4OME's complexes were confirmed to have an octahedral geometry as shown in Figure 3.

Electronic Spectra

The UV–vis spectra of SB4OME and its metal complexes data are given in Table 4. The SB4OME's spectrum shows high intensity bands observed at 259 and 281 nm which is corresponding to the $\pi \rightarrow \pi^*$ and $n \rightarrow \pi^*$ transitions of the benzene rings respectively [27]. Upon complexation, they do not significantly change in their absorption bands at 256-273 nm.

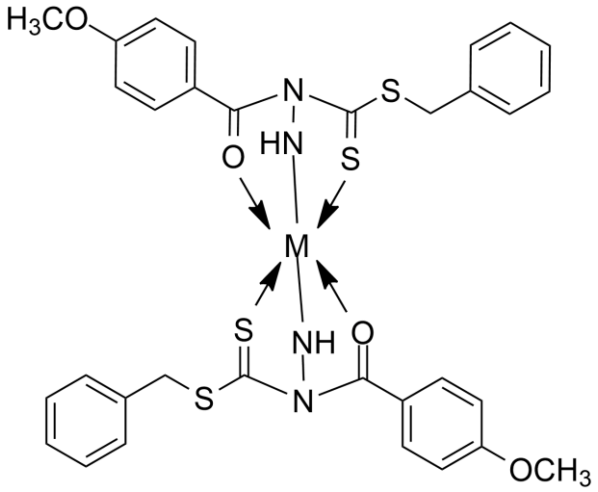

M = Cu, Zn, Co and Ni

Figure 3. Octahedral geometry of SB4OME's complexes.

Table 4. UV–Vis, molar conductivity data and magnetic moment data of SB4OME and its metal complexes.

Compound	λ_{max}, *nm (log ε, cm^{-1} mol^{-1} L)*	*Molar conductivity (ohm^{-1} mol^{-1} cm^{2})*	μ_{eff} *(B.M.)*
SB4OME	281 (4.134), 259 (4.116)	-	-
$Cu(SB4OME)_2$	554 (2.605), 327 (3.763), 268 (3.904)	31.4	1.648
$Zn(SB4OME)_2$	326 (3.503), 258 (3.573)	33.6	diamagnetic
$Co(SB4OME)_2$	624 (2.176), 326 (3.403), 260 (3.627)	32.4	4.740
$Ni(SB4OME)_2$	720 (2.017), 555 (2.315), 391 (3.441), 273 (3.864)	37.8	2.385

However, they show a bathochromic shift relative to its free ligand at 326 to 391 nm which is an indication of the complexation by SB4OME and in accordance with the results of the other spectral data. The properties of metal ions have a significant impact on the position of the absorption band. The modern molecular orbital theory states that certain factors that can influence the electronic density of a conjugated system must cause a bathochromic or hypochromic shift of the absorption bands [28]. The electro-negativity of the various metal ions in metal complexes with the same ligand is typically a major contributor to bathochromic shifts [29]. Only Zn(II) complex did not show any presence of low intensity band at 500 to 800 nm which is considered to arise from the forbidden $d \rightarrow d$ transition [2]. Copper(II) and cobalt(II) complex showed a broad peak at 554 and 624 nm assigned to $^2E_g \rightarrow {}^2T_{2g}$ and $^4T_{1g}(F) \rightarrow {}^4T_{2g}(F)$ transition respectively suggesting an octahedral geometry [25]. Furthermore, $Ni(SB4OME)_2$ displayed two low energy $d \rightarrow d$ transitions at 720 and 555 nm assigned to $^3A_{2g} \rightarrow {}^3T_{2g}(F)$ and $^3A_{2g} \rightarrow {}^3T_{1g}(F)$ respectively indicating an octahedral geometry of nickel complex [30].

Antimicrobial Assay

The results of the minimum inhibition concentration are shown in Table 5 along with the corresponding positive controls. Positive controls (gentamycin) demonstrated an excellent growth inhibition (MIC=<109 µg/ml) against each of the four tested organisms. SB4OME shows moderate activity (MIC=875 µg/ml) against all bacteria except *Pseudomonas aeruginosa* (MIC=1750 µg/ml). The activity was reduced compared to its precursor, SBDTC, which might be due to the presence of benzyl group which rendered it high activity [13].

The data in Table 5 clearly shows that all the compounds' antibacterial effectiveness increased with complexation against all types of bacteria except for *Bacillus cereus*. All the complexes exhibited approximately twice the inhibiting activity compared to the activity of SBDTC and SB4OME against *S. aureus*. The potency of SB4OME with its complex remains the same against Bacillus cereus (MIC=875 µg/ml). Nevertheless, the observed increase in metal complex efficacy against other bacteria can be attributed to major physicochemical changes in the compounds that occur during chelation. For instance, the presence of metal increased the compounds' molecular weight, changed their spatial geometry, and introduced new redox properties [31]. The polarity of the metal complex is also reduced more than its free ion as a result of the overlapping of the ligand orbital and partial sharing of the metal ion's positive charge with the donor groups [32]. Additionally, it increases the lipophilicity of complexes in aqueous solutions and encourages the delocalization of π-electrons across the entire chelate ring, which may alter the interactions of the compound with biological membranes [33-35]. The alterations to the metal complexes may also make them compatible with the hydrophobic pocket at the target site of the bacteria, strengthening their ability to bind to the microbe and resulting in higher penetration and an increase in their bioactivity [36-37].

Despite having better antibacterial activity than their ligand, all complexes showed a similar pattern for MIC value in each bacterium even with different metals used. Only $Zn(SB4OME)_2$ inhibit different concentrations (MIC=1750 µg/ml) against *P. aeruginosa* compared to other metal complexes, showing the insignificant effect of different metals in its anti-bacterial activity. The findings also indicate that all complexes also selectively inhibit *Staphylococcus aureus* and *Escherichia coli* more severely compared to *Bacillus cereus* and *Pseudomonas aeruginosa*. It is different from other significant findings which usually the Gram-positive bacteria were inhibited more severely than Gram-negative bacteria [32]. This can be explained by considering both bacterial species' structural characteristics. It has been discovered that gram-negative bacteria have an additional, very impermeable layer on top of the peptidoglycan [38]. Teichoic acids, a type of polysaccharide found in the cell wall of Gram-positive bacteria, are negatively charged and have helped the passage of positive metal ions [31].

Table 5. Antimicrobial activity of SB4OME ligand and its metal complexes.

Compound	***MIC (ug/ml)***			
	Gram-positive bacteria		Gram-negative bacteria	
	S. aureus (ATCC 25923)	*B. cereus* (ATCC 11778)	*E. coli* (ATCC 25922)	*P. aeruginosa* (ATCC 27853)
SBDTC	875	437	437	875
SB4OME	875	875	875	1750
$Cu(SB4OME)_2$	437	875	437	875
$Zn(SB4OME)_2$	437	875	437	1750
$Co(SB4OME)_2$	437	875	437	875
$Ni(SB4OME)_2$	437	875	437	875
Gentamycin	<109	<109	<109	<109

Assessment of Drug-likeness and ADMET Analysis

Due to poor absorption, distribution, metabolism, excretion, and toxicity issues of compounds generated from dithiocarbazate, most leads are unable to reach the market. In this study, drug-likeness and ADMET profiles of SBDTC, SB4OME with and without metal complexes were investigated (Table 7). The drug-likeness was assessed by Lipinski's rule of five (RO5) while ADMET analysis was by SwissADME and Protox-II. The Lipinski parameters help determine whether substances are able to effectively penetrate biological systems and be absorbed, leading to good oral bioavailability [39]. Desirable drug candidates must meet at least four of the five criteria, which include (a) the number of hydrogen bond acceptor groups less than 10; (b) the number of hydrogen bond donor groups does not exceed 5 (c) the molecular weight less than 500; (d) the octanol-water partition coefficient that does not exceed 5 and; (e) the topological polar surface area less than 140 $Å^2$ [40]. SwissADME analyses the ADME properties by considering a few parameters which include molecular weight, topological surface area (TPSA) and several rotatable bonds (ntrob). The number of rotatable bonds should be less than 10 to control conformational alterations and for oral bioavailability [41-43].

Following Lipinski's rule, the precursor, SBDTC with its modification, SB4OME demonstrated the potential of good permeability and absorption with zero violation. Additionally, they also showed excellent bioavailability according to the bioavailability radar (Table 6) where most of the parameters were within the optimal range. However, despite having good activity in their antimicrobial assay, all complexes show few violations from Lipinski's rule and ADME analysis including exceeding molecular weight of 500 g/mol and TPSA of more than 140 $Å^2$. The value for both violations was doubled for all complexes compared to its free ligand due to the ratio of metal to a ligand which is 1:2. As a result, all parameters observed were not within the optimal range as shown in Table 6. Furthermore, RO5 has limitations whereby it only fit the criteria for small molecule, but not the complexes or larger molecule such as antibody and protein [44]. Nevertheless, all compounds under investigation have a good bioavailability score. Compounds having positive drug-likeness scores should be regarded as drugs and all the examined compounds displayed positive values of 0.55, so they seem to be drug-like [45].

Table 6. Bioavailability radar of SBDTC, SB4OME and its complexes.

Compound	***SBDTC***	***SB4OME***	***Complexes***
Bioavailability radar	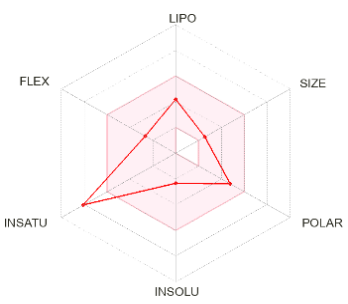	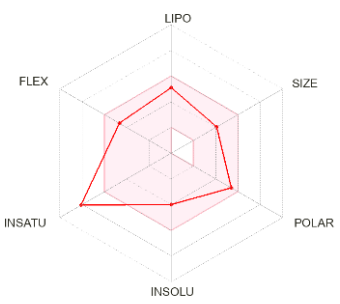	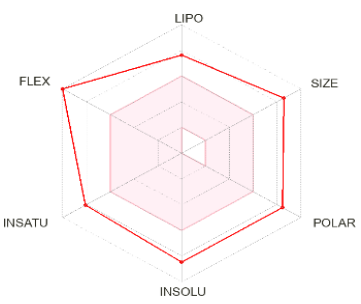

Table 7. Prediction of ADMET properties.

Parameter	***SBDTC***	***SB4OME***	***Cu(SB4OME)$_2$***	***Zn(SB4OME)$_2$***	***Co(SB4OME$_2$***	***Ni(SB4OME)$_2$***
Molecular weight (g/mol)	198.31	332.44	724.4	728.23	721.78	721.54
Log *P*	1.66	2.78	4.13	4.13	4.13	4.13
H-bond acceptors	1	2	6	6	6	6
H-bond donors	2	2	2	2	2	2
Lipinski's violation	0	0	1	1	1	1
TPSA	95.44	107.75	197.92	197.92	197.92	197.92
Rotatable bond	4	8	18	18	18	18
Bioavailability score	0.55	0.55	0.55	0.55	0.55	0.55
LD_{50} (mg/kg)	300	1500	2050	1500	1500	2050
Toxicity class	3	4	5	4	4	5
Carcinogenicity	active	inactive	inactive	inactive	inactive	inactive
Immunotoxicity	inactive	inactive	inactive	inactive	inactive	inactive
Mutagenicity	active	inactive	active	active	active	active
Cytotoxicity	inactive	inactive	inactive	inactive	inactive	inactive

Based on a toxicity risk assessment, SB4OME has a good toxicity profile with the predicted LD_{50} of 1500 mg/kg, putting it in toxicity class 4. A similar toxicity class was shown by Zn(II) and Co(II) complex while Cu(II) and Ni(II) showed the least toxicity risk with LD_{50} of 2050 mg/kg, putting it in toxicity class 5. As expected, SBDTC showed the most toxic compound with LD_{50} of 300 mg/kg which is regarded as category 3. Although toxicity class 4 and 5 is less toxic compared to class 3, they were still acceptable for new drugs [46]. According to the median lethal dose value (LD_{50}), all the synthesized compounds, SB4OME and its complexes predicted to be at least five times safer or less toxic compared to its precursor, SBDTC, although they proved to have similar or better antibacterial activity. Further toxicity assessments were done on all compounds to determine their carcinogenicity, immunotoxicity, mutagenicity and cytotoxicity (Table 7). The results indicated that SB4OME was the safest compound with non-carcinogenic in nature and has no influence on immunotoxicity, mutagenicity and cytotoxicity while its complexes were only active in mutagenicity. SBDTC, on other hand, was carcinogenic and active in mutagenicity. Toxicity analysis concluded that modification at SBDTC lowered the risk of toxicity as shown by SB4OME and its complexes.

CONCLUSION

In conclusion, the new substituted dithiocarbazates derivative, *S*-benzyl-α-*N*-(anisoyl) dithiocarbazate (SB4OME) which derived from the condensation of *S*-benzyldithiocarbazate with 4-benzoylchloride, behaves as a uninegative tridentate ligand with its ONS donor set to form bis-chelated Cu(II), Zn(II), Co(II) and Ni(II) complexes. Through the spectral data, SB4OME was found to exist as thione in both solid and solution. SB4OME was moderately active (MIC = 875 µg/ml) against *S. aureus*, *B. cereus* and *E. coli* and the bioactivity was enhanced upon complexation. Moreover, the synthesized compounds mostly followed the parameters of Lipinski's rule of five, showed good ADME properties and had a good toxicity profile. Thus, in this project, considering their effectiveness in biological activity, ADME profile and toxicity risk, $Cu(SB4OME)_2$ and $Ni(SB4OME)_2$ complex were the best compounds that could be potential drug candidates and may be considered for further drug development.

ACKNOWLEDGMENTS

The authors thank the Department of Chemistry, Kulliyyah of Science, International Islamic University Malaysia Kuantan for the provision of laboratory facilities. An appreciation was also given to Associate Professor Dr. Nadiah Halim from Universiti Malaya for her help in magnetic susceptibility analysis.

The authors declare that they have no conflict of interest.

REFERENCES

1. Sohtun, W. P., Kathiravan, A., Asha Jhonsi, M., Aashique, M., Bera, S. & Velusamy, M. (2022) Synthesis, crystal structure, BSA binding and antibacterial studies of Ni(II) complexes derived from dithiocarbazate based ligands. *Inorganica Chimica Acta*, **536**, 120888.

2. Bhat, R. A., Singh, K., Kumar, D., Kumar, A. & Mishra, P. (2022) Antimicrobial studies of the Zn(II) complex of *S*-benzyl-β-(*N*-2-methyl-3-

phenylallylidene)dithiocarbazate. *Journal Of Coordination Chemistry*, **75(7–8)**, 1050–1062.

3. Md Yusof, E. N., Latif, M. A. M., Tahir, M. I. M., Sakoff, J. A., Veerakumarasivam, A., Page, A. J., Tiekink, E. R. T. & Ravoof, T. B. S. A. (2020) Homoleptic tin(IV) compounds containing tridentate ONS dithiocarbazate Schiff bases: Synthesis, X-ray crystallography, DFT and cytotoxicity studies. *Journal of Molecular Structure*, **1205**, 127635.

4. Ramilo-Gomes, F., Addis, Y., Tekamo, I., Cavaco, I., Campos, D. L., Pavan, F. R., Gomes, C. S. B., Brito, V., Santos, A. O., Domingues, F., Luís, Â., Marques, M. M., Pessoa, J. C., Ferreira, S., Silvestre, S. & Correia, I. (2021) Antimicrobial and antitumor activity of *S*-methyl dithiocarbazate Schiff base zinc(II) complexes. *Journal of Inorganic Biochemistry*, **216**.

5. Cavalcante, C. D. Q. O., Arcanjo, D. D. S., Silva, G. G. D., Oliveira, D. M. D. & Gatto, C. C. (2019) Solution and solid behavior of mono and binuclear Zinc(II) and Nickel(II) complexes with dithiocarbazates: X-ray analysis, mass spectrometry and cytotoxicity against cancer cell lines. *New Journal of Chemistry*, **43(28)**, 11209–11221.

6. Rosnizam, A. N., Hamali, M. A., Muhammad Low, A. L., Anouar, E. H., Youssef, H. M., Bahron, H. & Mohd Tajuddin, A. (2022) Palladium(II) complexes bearing N,O-bidentate Schiff base ligands: Experi-mental, in-silico, antibacterial, and catalytic properties. *Journal of Molecular Structure*, **1260**, 132821.

7. Kargar, H., Ashfaq, M., Fallah-Mehrjardi, M., Behjatmanesh-Ardakani, R., Munawar, K. S. & Tahir, M. N. (2022) Unsymmetrical Ni(II) Schiff base complex: Synthesis, spectral characterization, crystal structure analysis, Hirshfeld surface investigation, theoretical studies, and anti-bacterial activity. *Journal of Molecular Structure*, **1265**, 133381.

8. Chabicovsky, M., Prieschl-Grassauer, E., Seipelt, J., Muster, T., Szolar, O. H. J., Hebar, A. & Doblhoff-Dier, O. (2010) Pre-clinical safety evaluation of pyrrolidine dithiocarbamate. *Basic and Clinical Pharmacology and Toxicology*, **107(3)**, 758–767.

9. Pal, T. K., Mumit, M. A., Hossen, J., Paul, S., Alam, M. A., Islam, M. A. A. A. A. & Sheikh, M. C. (2021) Computational and experimental insight into antituberculosis agent, (E)-benzyl-2-(4-hydroxy-2-methoxybenzylidene) hydrazine-carbodithioate: ADME analysis. *Heliyon*, **7(10)**, e08209.

10. Lipinski, C. A. (2004) Lead- and drug-like compounds: the rule-of-five revolution. *Drug Discovery Today: Technologies*, **1(4)**, 337–341.

11. Drwal, M. N., Banerjee, P., Dunkel, M., Wettig, M. R. & Preissner, R. (2014) ProTox: a web server for the in-silico prediction of rodent oral toxicity. *Nucleic Acids Research*, **42**, W53.

12. Ali, M. A. & Bose, R. (1977) Metal complexes of schiff bases formed by condensation of 2-methoxybenzaldehyde and 2-hydroxybenzalde-hyde with *S*-benzyldithiocarbazate. *Journal of Inorganic and Nuclear Chemistry*, **39**, 265-269.

13. How, F. N. F., Crouse, K. A., Tahir, M. I. M., Tarafder, M. T. H. & Cowley, A. R. (2008) Synthesis, characterization and biological studies of S-benzyl-β-*N*-(benzoyl) dithiocarbazate and its metal complexes. *Polyhedron*, **27(15)**, 3325–3329.

14. Malmberg, C., Yuen, P., Spaak, J., Cars, O., Tängdén, T. & Lagerbäck, P. (2016) A Novel Microfluidic Assay for Rapid Phenotypic Antibiotic Susceptibility Testing of Bacteria Detected in Clinical Blood Cultures. *Plos One*, **11(12)**, e0167356.

15. Gwaram, N. S., Ali, H. M., Khaledi, H., Abdulla, M. A., Hadi, H. A., Lin, T. K., Ching, C. L. & Ooi, C. L. (2012) Antibacterial evaluation of some schiff bases derived from 2-acetylpyridine and their metal complexes. *Molecules*, **17(5)**, 5952–5971.

16. Daina, A., Michielin, O. & Zoete, V. (2017) SwissADME: a free web tool to evaluate pharmacokinetics, drug-likeness and medicinal chemistry friendliness of small molecules. *Scientific Reports*, **7**.

17. Banerjee, P., Eckert, A. O., Schrey, A. K. & Preissner, R. (2018) ProTox-II: a webserver for the prediction of toxicity of chemicals. *Nucleic Acids Research*, **46**, W257.

18. Akbar Ali, M. & Tarafdar, M. T. H. (1977) Metal complexes of sulphur and nitrogen-containing ligands: Complexes of *S*-benzyldithiocarbazate and a schiff base formed by its condensation with pyridine-2-carboxaldehyde. *Journal of Inorganic and Nuclear Chemistry*, **39(10)**, 1785–1791.

19. Solomons T. W. G., Fryhle, C. B. & Snyder, S. A. (2016) *Organic Chemistry*, **1124**.

20. Tarafder, M. T. H., Khoo, T. J., Crouse, K. A., Ali, A. M., Yamin, B. M. & Fun, H. K. (2002) Coordination chemistry and bioactivity of some metal complexes containing two isomeric

bidentate NS Schiff bases derived from S-benzyldithiocarbazate and the X-ray crystal structures of *S*-benzyl-β-*N*-(5-methyl-2-furyl-methylene) dithiocarbazate and bis[*S*-benzyl-β-*N*-(2-furylmethylketone)dithiocarbazato] cadmium (II). *Polyhedron*, **21(27–28)**, 2691–2698.

21. Ali, I., Wani, W. A. & Saleem, K. (2013) Empirical formulae to molecular structures of metal complexes by molar conductance. *Synthesis and Reactivity in Inorganic, Metal-Organic and Nano-Metal Chemistry*, **43(9)**, 1162–1170.

22. Wahba, M., El-Tabl, A. S., Abd-El Wahed, M. M., Wahba, M. A., EL-assaly, S. A. & Saad, L. M. (2014) Sugar Hydrazone Complexes; Synthesis, Spectroscopic Characterization and Antitumor Activity Some of the authors of this publication are also working on these related projects: bioinorganic application View project Metal oxides for pharmaceutical application View project Sugar Hydrazone Complexes; Synthesis, Spectroscopic Characterization and Antitumor Activity. *Journal of Advances in Chemistry*, **9(1)**.

23. Emam, S. M., El-Saied, F. A., Abou El-Enein, S. A. & El-Shater, H. A. (2009) Cobalt(II), nickel(II), copper(II), zinc(II) and hafnium(IV) complexes of N′-(furan-3-ylmethylene)-2-(4-methoxyphe nylamino)acetohydrazide. *Spectrochimica Acta Part A: Molecular and Biomolecular Spectroscopy*, **72(2)**, 291–297.

24. Abdalrazaq, E. A., Al-Ramadane, O. M. & Al-Numa, K. S. (2010) Synthesis and characterization of dinuclear metal complexes stabilized by tetradentate schiff base ligands. *American Journal of Applied Sciences*, **7(5)**, 628–633.

25. Xuan Hung, N., Anh Quang, D., Thanh Tam Toan, T. al, Hamza Abbas, S., Mohammad Ali Murad, D., Hamza Abbas, H., Mahmoud, W. A. M., Hassan, Z. & Russel, W., Ali (2020) Synthesis and spectral analysis of some metal complexes with mixed Schiff base ligands 1-[2-(2-hydroxybenzylidene amino)ethyl]pyrrolidine-2,5-dione (HL1) and (2-hydroxybenzalidine)glycine (HL2). *Journal of Physics: Conference Series*, **1660(1)**, 012027.

26. Lever, A. B. P. (1984) Inorganic electronic spectroscopy. *Studies in Physical and Theoretical Chemistry*, **33**, 861-863.

27. Guo, L., Wu, S., Zeng, F. & Zhao, J. (2006) Synthesis and fluorescence property of terbium complex with novel schiff-base macromolecular ligand. *European Polymer Journal*, **42(7)**, 1670–1675.

28. Kasumov, V. T. & Köksal, F. (2003) Synthesis, spectroscopic characterization and redox reactivity of the copper(II) salicylaldiminates containing sterically hindered 2,6-diphenylphenol. *Transition Metal Chemistry*, **28(8)**, 888–892.

29. Chen, Z., Wu, Y., Gu, D. & Gan, F. (2007) Spectroscopic, and thermal studies of some new binuclear transition metal(II) complexes with hydrazone ligands containing acetoacetanilide and isoxazole. *Spectrochimica Acta Part A: Molecular and Biomolecular Spectroscopy*, **68(3)**, 918–926.

30. El-Samanody, E. S. A., AbouEl-Enein, S. A. & Emara, E. M. (2018) Molecular modeling, spectral investigation and thermal studies of the new asymmetric Schiff base ligand; (E)-N'-(1-(4-((E)-2-hydroxybenzylideneamino)phenyl) ethylidene) morpholine-4-carbothiohydrazide and its metal complexes: Evaluation of their antibacterial and anti-molluscicidal activity. *Applied Organometallic Chemistry*, **32(4)**, e4262.

31. Low, M. L. (2014) Synthesis, characterization and bioactivites of dithiocarbazate Schiff base ligands and their metal complexes. *Ph.D. Thesis, Universiti Putra Malaysia, Malaysia*.

32. Break, M. K. bin, Tahir, M. I. M., Crouse, K. A. & Khoo, T. J. (2013) Synthesis, characterization, and bioactivity of schiff bases and their Cd^{2+}, Zn^{2+}, Cu^{2+}, and Ni^{2+} complexes derived from chloroacetophenone isomers with *S*-benzyldithiocarbazate and the X-ray crystal structure of *S*-benzyl-β-*N*-(4-chlorophenyl) methylenedithiocarbazate. *Bioinorganic Chemistry and Applications.*

33. Raman, N., Muthuraj, V., Ravichandran, S. & Kulandaisamy, A. (2003) Synthesis, characterisation and electrochemical behaviour of Cu(II), Co(II), Ni(II) and Zn(II) complexes derived from acetylacetone andp-anisidine and their antimicrobial activity. *Journal of Chemical Sciences*, **115(3)**, 161–167.

34. Tiwari, K. N., Monserrat, J. P., Hequet, A., Ganem-Elbaz, C., Cresteil, T., Jaouen, G., Vessières, A., Hillard, E. A. & Jolivalt, C. (2012) In vitro inhibitory properties of ferrocene-substituted chalcones and aurones on bacterial and human cell cultures. *Dalton Transactions*, **41(21)**, 6451–6457.

35. Lobana, T. S., Sharma, R., Bawa, G. & Khanna, S. (2009) Bonding and structure trends of thiosemicarbazone derivatives of metals—An overview. *Coordination Chemistry Reviews*, **253(7–8)**, 977–1055.

36. Ming, L. J. (2003) Structure and function of "metalloantibiotics. *Medicinal Research Reviews*, **23(6)**, 697–762.

37. Efthimiadou, E. K., Katsarou, M. E., Karaliota, A. & Psomas, G. (2008) Copper(II) complexes with sparfloxacin and nitrogen-donor heterocyclic ligands: Structure–activity relationship. *Journal of Inorganic Biochemistry*, **102(4)**, 910–920.

38. Silhavy, T. J. (2016) Classic Spotlight: Gram-Negative Bacteria Have Two Membranes. *Journal of Bacteriology*, **198(2)**, 201.

39. Schyman, P., Liu, R., Desai, V. & Wallqvist, A. (2017) vNN web server for ADMET predictions. *Frontiers in Pharmacology*, **8(889)**.

40. Castillo-Morales, R. M., Carreño Otero, A. L., Mendez-Sanchez, S. C. da Silva, M. A. N., Stashenko, E. E., & Duque, J. E. (2019) Mitochondrial affectation, DNA damage and AChE inhibition induced by Salvia officinalis essential oil on Aedes aegypti larvae. *Comparative Biochemistry and Physiology Part C: Toxicology & Pharmacology*, **221**, 29–37.

41. Ghose, A. K., Herbertz, T., Hudkins, R. L., Dorsey, B. D. & Mallamo, J. P. (2012) Knowledge-Based, Central Nervous System (CNS) Lead Selection and Lead Optimization for CNS Drug Discovery. *ACS Chemical Neuroscience*, **3(1)**, 50–68.

42. Lipinski, C. A., Lombardo, F., Dominy, B. W. & Feeney, P. J. (1997) Experimental and computational approaches to estimate solubility and permeability in drug discovery and development settings. *Advanced Drug Delivery Reviews*, **23(1–3)**, 3–25.

43. Veber, D. F., Johnson, S. R., Cheng, H. Y., Smith, B. R., Ward, K. W. & Kopple, K. D. (2002) Molecular properties that influence the oral bioavailability of drug candidates. *Journal of Medicinal Chemistry*, **45(12)**, 2615–2623.

44. Benet, L. Z., Hosey, C. M., Ursu, O. & Oprea, T. I. (2016) BDDCS, the Rule of 5 and Drugability. *Advanced Drug Delivery Reviews*, **101**, 89.

45. Gad, E. M., Nafie, M. S., Eltamany, E. H., Hammad, M. S. A. G., Barakat, A., Barakat, A. & Boraei, A. T. A. (2020) Discovery of New Apoptosis-Inducing Agents for Breast Cancer Based on Ethyl 2-Amino-4,5,6,7-Tetra Hydrobenzo [β]Thiophene-3-Carboxylate: Synthesis, In Vitro, and In Vivo Activity Evaluation. *Molecules*, **25(11)**, 2523.

46. Xiao, L. L., Zhang, F., Zhao, Y. L., Zhang, L. J., Xie, Z. Y., Huang, K. Z., Ouyang, X. X., Wu, X. X., Xu, X. W. & Li, L. J. (2020) Using advanced oxidation protein products and ischaemia-modified albumin to monitor oxidative stress levels in patients with drug-induced liver injury. *Scientific Reports*, **10(1)**, 1–10.